

# Switchable topological domains in point contacts based on transition metal tellurides

Yu. G. Naidyuk<sup>1\*</sup>, D. L. Bashlakov<sup>1</sup>, O.E. Kvitnitskaya<sup>1</sup>, B. R. Piening<sup>2</sup>, G. Shipunov<sup>2</sup>,  
D. V. Efremov<sup>2\*</sup>, S. Aswartham<sup>2</sup>, B. Büchner<sup>2,3</sup>

<sup>1</sup>*B. Verkin Institute for Low Temperature Physics and Engineering, NAS of Ukraine, 61103 Kharkiv, Ukraine*

<sup>2</sup>*Institute for Solid State Research, IFW Dresden, D-01171 Dresden, Germany*

<sup>3</sup>*Institute of Solid State and Materials Physics, TU Dresden, D-01062 Dresden, Germany*

## Abstract

Resistive switching in voltage biased point contacts (PCs) based on series of transition metals tellurides (TMTs) such as  $MeTe_2$  ( $Me=Mo, W$ ) and  $TaMeTe_4$  ( $Me= Ru, Rh, Ir$ ) has been observed. The switching occurs between a low resistive “metallic-type” state and a high resistive “semiconducting-type” state by applying certain bias voltage ( $<1V$ ), while reverse switching takes place by applying voltage of opposite polarity. The switching effect consists in changing the PC resistance up to two orders of magnitude, which increases with decreasing temperature. The origin of the effect can be formation of domain in PC core by applying a bias voltage, when a strong electric field (about  $10kV/cm$ ) modifies crystal structure and/or control its polarization. Besides, impact of domain wall with topological interfacial states is also considered. Thus, we demonstrate the new functionality of studied TMTs arising from switchable domains in submicron hetero-structures, that is promising, e. g., for non volatile RRAM engineering.

---

\*Corresponding authors: [naidyuk@ilt.kharkov.ua](mailto:naidyuk@ilt.kharkov.ua); [d.efremov@ifw-dresden.de](mailto:d.efremov@ifw-dresden.de)

## Introduction

Layered van der Waals transition metal chalcogenides (TMC) attract a lot of attention in the scientific community both due to the manifestation of their remarkable electronic properties, which can be modified by element composition, crystal structure, thickness, electronic density etc. and possibility of their use in potential nanoelectronic and spintronic applications (see [1] and Refs. therein). During the last decade, an enormous attention to TMC compounds associated with the theoretical prediction that, some of them (e.g.,  $\text{MoTe}_2$ ,  $\text{WTe}_2$ ) can be Weyl semimetals possessing of massless fermionic excitations and topologically robust electronic surface states [2]. On the other hand, layered structure of TMC with a weak van der Waals binding between layers allows exfoliate these materials up to monolayers. The latter opens an amazing window to observe new size dependent properties in TMC and allows take advantage of this opportunity in future applications [3].

We recently explored two of TMC, namely  $\text{MoTe}_2$  [4] and  $\text{WTe}_2$  [5], by using of point contact (PC) technique [6]. This method also allows us to study properties of materials in restricted geometry from submicron to nanometer scale under high current density and electric field. Importantly, that interface properties have impact on PC conductivity, what represents of special interest at study of TMC, where exotic Fermi-arc with topologically protected surface states are expected and utilizing of topological surface states remains challenging. It is also known, that phase transition can be detected by measuring of nonlinear conductivity of PCs, as it was shown for the first time for ferromagnetic metals [7]. Motivated by mentioned abilities of PC technique and using the fact that  $\text{MoTe}_2$  undergoes a first-order structural phase transition from the monoclinic  $1T'$  to the orthorhombic  $T_d$  (both semimetallic) phase at a temperature of about 250K [8], we started looking for the manifestation of this transition and other potential effects in  $\text{MoTe}_2$  applying to PCs high voltages. As a result, bi-stable resistive states with reversible switching in current-voltage  $I$ - $V$  characteristics of  $\text{MoTe}_2$  PCs at biases of several hundreds of millivolts were discovered. The similar effect has been registered also for PCs based on related TMCs like  $\text{WTe}_2$ ,  $\text{TaRuTe}_4$ ,  $\text{TaRhTe}_4$  and  $\text{TaIrTe}_4$ . The observed bipolar resistive switching in devices based on studied series of TMC compounds, regardless of its inner nature, is of great importance and could be applicable to create a new type of resistive random-access memory (RRAM) devices as potential alternatives to existing nonvolatile memories. Additionally, along with this discovery, the understanding underlying physics of processes is of particular interest, while utilizing of topological properties and surface states at interface in TMCs pave the way to nanoelectronics with astonishing functionalities.

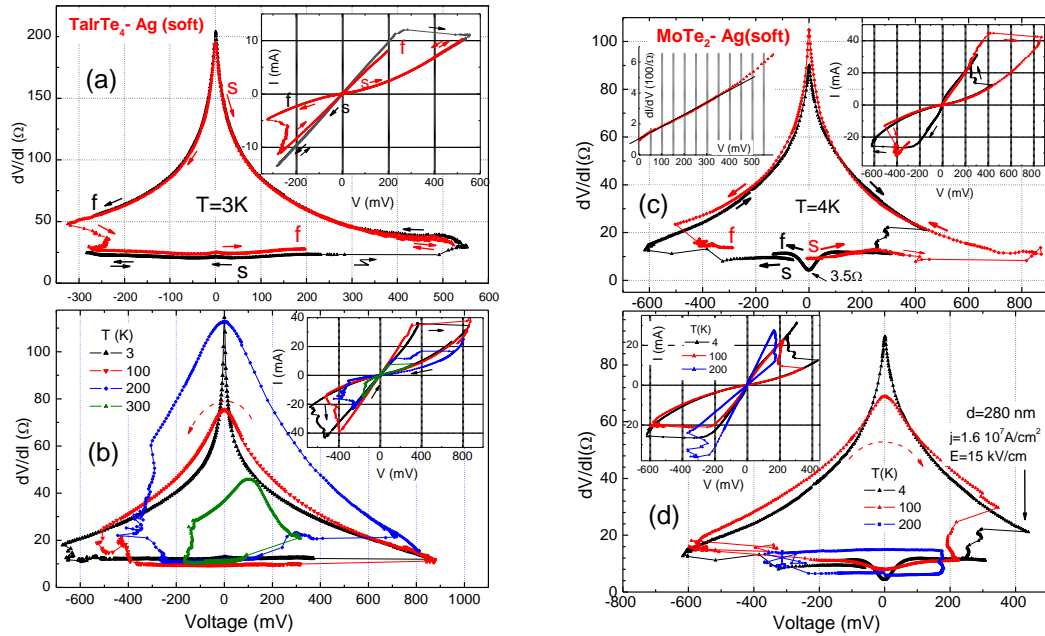
## Experimental results

Figure 1 shows  $dV/dI$  and  $I$ - $V$  (in insets) characteristics of “soft” PCs  $\text{TaIrTe}_4$  and  $\text{MoTe}_2$  PCs, respectively. A closed loop for  $dV/dI$  and a butterfly shape for  $I$ - $V$  behavior are seen for these characteristics by sweeping bias voltage from one to opposite polarity and back. For example, starting from the low resistance state (LRS), switching to the high resistance state (HRS) occurs above +250 mV (Fig.1(a), black curve), while by sweeping LRS to the opposite negative bias no switching is observed. At the same time, starting from the HRS (Fig.1(a), red curve), where  $dV/dI$  demonstrate sharp zero-bias maximum, transition to the LRS takes place only at negative polarity, a bit above -300mV, while at positive polarity no switching to LRS is observed up to +520 mV.

Figure 1(b) shows  $dV/dI$  and  $I$ - $V$  (in inset) characteristics of another “soft” PC based on  $\text{TaIrTe}_4$  at different temperatures. Here, the switching effect persists up to the room temperature, only amplitude of zero bias  $dV/dI$  maximum goes down and switching voltage decreases.

Figure 1(c) demonstrates similar dependences for two  $\text{MoTe}_2$  PCs. Here, the switching LRS to HRS is at positive polarity for a red curve, like for PC from Fig. 1(a), while for another

PC (black curve) the switching LRS to HRS (or HRS to LRS) is at negative (positive) polarity. Figure 1(d) shows evolution of  $dV/dI$  and  $I-V$  (in inset) characteristics of the latter PC with temperature, where amplitude of the effect and switching voltage decreases. The diameter of this PC was estimated as 280 nm using temperature dependence of their zero bias resistance analogously as it was made in Supplement of Ref. [5]. Using diameter, strength of the electric field about 15 kV/cm and the current density  $1.6 \cdot 10^7$  A/cm<sup>2</sup> were estimated at, e.g., HRS to LRS transition.



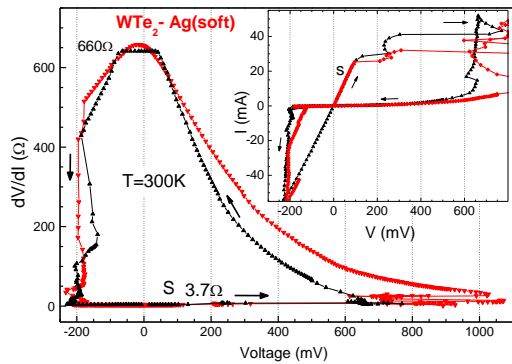
**Figure 1.** Differential resistance and  $I-V$  curves behavior for “soft” contacts based on TMC at different temperatures. (a)  $dV/dI$  of “soft” contacts TaIrTe<sub>4</sub>-Ag measured at 3K starting from LRS (black curve) and HRS (red curve). “s” marks the start of measurements and “f” is for the finish, arrows show direction of the current sweep. The black curve is measured starting towards negative voltages - forth and back, while transition to HRS occurs only at positive voltages. The red curve is measured starting towards positive voltages - forth and back, while transition to LRS occurs only at negative voltages. Inset shows  $I-V$  curves corresponding to  $dV/dI$  from the main panel. (b)  $dV/dI$  of another “soft” contact TaIrTe<sub>4</sub>-Ag measured at different temperatures. The curves are measured “counterclockwise”. Inset shows  $I-V$  curves corresponding to  $dV/dI$  from the main panel. (c)  $dV/dI$  of two (black and red) “soft” contacts MoTe<sub>2</sub>-Ag measured starting from LRS. “s” marks the start of measurements and “f” is for the finish. Arrows show direction of the current sweep. Transition from the LRS to HRS (or from the HRS to LRS) occurs at opposite polarities for these two contacts. Right inset shows  $I-V$  curves corresponding to  $dV/dI$  from the main panel. Left inset shows that the differential conductivity  $dI/dV$  for contact from the main panel displays a clear linear relationship<sup>1</sup>. (d)  $dV/dI$  of 3.5  $\Omega$  “soft” contact from the main panel measured at different temperatures. The diameter of this contact was estimated as 280 nm using temperature dependence of their zero bias resistance analogously as it was made in Supplement of Ref. [5]. Using diameter, strength of electric field and current density were estimated at HRS to LRS transition (shown by arrow).

Figure 2 shows  $dV/dI$  and  $I-V$  (in inset) characteristics of PC with WTe<sub>2</sub> at room temperature, where difference in the resistance between LRS and HRS reaches more than two orders of magnitude (see also Figs. S8 in Supplement in the case of MoTe<sub>2</sub>). There is instability in  $I-V$  at LRS to HRS transition above 150 mV. At the same, time analogous transition at helium temperature is quite sharp (see, e.g., Fig. 1). This is apparently connected with enhanced fluctuation at structural transition at higher temperature. Figure 2 demonstrates also comparison of  $dV/dI$  for the same PC measured with time interval of about 12 hours to show their reproducibility (or stability of switching effect under ambient conditions).

<sup>1</sup> Similar linear part in  $dI/dV$  at HRS is also seen for other compounds (see Figs. S5, S6, S7 in Supplement). It can also be seen here that  $dV/dI$  has a logarithmic behavior for a certain bias range. This observation is interesting and must be taken into consideration at developing of model of switching effect.

Similar switching effects were observed also for TaRhTe<sub>4</sub> and TaRuTe<sub>4</sub> (see Figs. S1 and S2 in Supplement). “Hard” PCs, where instead of silver paint a thin Ag wire was used, also demonstrate switching effect (see Figs. S2 and S3 in Supplement). A disadvantage of “hard” PCs is their weak mechanical stability, what makes difficult to keep them stable for a relative long time and especially by varying a temperature, therefore most measurements were carried out on “soft” PCs.

Figure 3 shows distribution of the switching voltages for LRS to HRS and HRS to LRS transitions for different PCs and for all compounds at helium and room temperatures. Here, the most data is present for MoTe<sub>2</sub> and TaIrTe<sub>4</sub> compounds (6 PCs for each compound). First of all, it is seen, that polarity of each transition (LRS to HRS or HRS to LRS) can be both positive and negative for different PCs with almost equal probability. For example, 3 PCs with MoTe<sub>2</sub> or TaIrTe<sub>4</sub> have LRS to HRS transition at positive polarity and 3 PCs at negative. However, if the switching occurs at a given polarity then it is absent at the opposite polarity, at least at the same bias voltage. Perhaps the atomic composition/termination of the upper layer (let's say Mo or Te) plays a role here. This point requires further investigation. Further, switching voltage has some distribution but is, on the average, smaller at a room temperature.



**Figure 2.** Differential resistance  $dV/dI$  and  $I$ - $V$  curves behavior for soft contact based on WTe<sub>2</sub> at room temperature. Two  $dV/dI$  of “soft” contact WTe<sub>2</sub>–Ag measured with time interval of 12 hours after storage this contact under ambient condition. “s” marks the start of measurements and arrows show direction of the current sweep. Note, the zero bias resistance is changed more than two order of magnitude. Inset shows  $I$ - $V$  curve corresponding to  $dV/dI$  from the main panel.

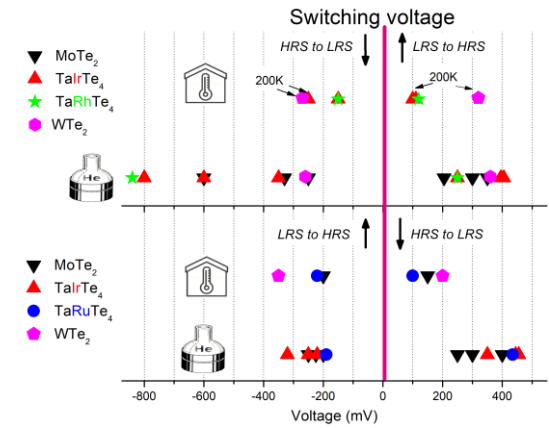


**Figure 3.** Distribution of the switching voltages for different PCs with studied compounds at helium (dewar) and room (box) temperatures. Upper (bottom) panel shows PCs where switching from LRS (HRS) to HRS (LRS) take place at positive (negative) voltage. Switching voltages for LRS to HRS transition are marked by up arrows and for HRS to LRS transition are marked by down arrows. For two PCs, switching voltages are shown at 200K (tilted arrows).

Finally, Figure S4 (in Supplement) demonstrates the detailed temperature dependence of  $dV/dI$ , where switching effect was measured for the first time. Here, the lack of switching at a low temperature was connected with necessity to apply a larger bias, while our setup has maximal current output of about 50 mA, therefore the maximal bias was limited by the low PC resistance. Detailed measurement of zero-bias resistance of this PC at different temperatures allowed us to estimate their size and, respectively, the electric field strength and current density. As a result, the estimated strength of an electric field at switching bias was about 2.5 times lower for this PC as compared to PC at helium temperature (see Fig. 1(d)). It should be noted, here that the estimation of the electric field gives it a lower value, since we assume the formation of single metallic contact or conducting channel. In the case of formation of several PCs their size will be smaller and the electric field will be correspondingly larger.

Note that  $dV/dI$  of MoTe<sub>2</sub> PC in LRS (see, e.g., black curve in Fig. 1 (c), (d) has “metallic” behavior at low voltages, which transforms to the “semiconducting-like” decrease of  $dV/dI$  at higher bias (see also Fig. S4 (a), (b) for more details) producing a distinct maximum in

$dV/dI$  around 200 mV similar to that what we observed in the case of  $\text{WTe}_2$  [5]. Interesting, that metallic to semiconducting like transition was observed around 200K in the temperature dependence of resistance of 6 nm thick  $\text{MoTe}_2$  sample (see Fig. 4S in Supplement of Ref. [9]). It seems that the reducing of the dimension promotes the emergence of a “semiconductor-like” behavior in  $\text{MoTe}_2$ .

### Discussion

Observed “bipolar” switching, from LRS to HRS (and opposite from HRS to LRS) occurs only at definite polarity. This unambiguously testifies in favor of the nonthermal mechanism. The switching occurs between “metallic-like” LRS and “semiconducting-like” HRS by applying a voltage above a certain threshold. That is a certain (phase) transition takes place in the PC at the interface when voltage is applied. Since thermal effects are disregarded, the only effect of electric field and/or high current density in our PCs must play a role.

Exploring the literature, we become aware of similar resistive switching observed by Zhang *et al.* [10] in “vertical devices made of  $\text{MoTe}_2$  and  $\text{Mo}_{1-x}\text{W}_x\text{Te}_2$  layers” (from 6 nm to 36 nm thick) sandwiched between metallic electrodes. Interestingly that the “active device area” (in average  $500 \times 400 \text{ nm}^2$ ) in [10] is close to the estimated size of PCs of several hundred nm (see Fig. 1(d) and S4 (c)). The Zhang *et al.* [10] explained switching supposing formation of a conductive filament with a transient structure (named  $2\text{H}_d$ ) after applying an electrical field. The  $2\text{H}_d$  phase, they considered as a distorted 2H phase, which exhibits electrical properties that range from semiconducting to metallic. Zhang *et al.* believe that  $\text{MoTe}_2$  (and  $\text{Mo}_{1-x}\text{W}_x\text{Te}_2$ ) undergo a reversible structural transition from a semiconducting 2H to a high (or more) conductive  $2\text{H}_d$  state.

Very recently, Datye *et al.* [11] reported the observation of similar switching in structure contained layered  $\text{MoTe}_2$  (10-55 nm thick) sandwiched between Au electrodes. They used scanning thermal microscopy to monitor temperature of the top Au electrode and observed hot spot of about  $1 \mu\text{m}$  size. They concluded that the switching “is likely caused by the breaking and forming of ... Au conductive plugs between the electrodes”, when significant Joule heating promotes Au migration.

Returning to our results, we must emphasize that, unlike Zhang *et al.* [10] and Datye *et al.* [11], we used “bulk” samples with thickness of about  $100 \mu\text{m}$  to create PCs. It makes unlikely formation of “conductive plug” from the electrode material, which is Ag in our case. Further, high (or more) conductive state (named here as LRS) demonstrates metallic behavior, as Fig. 1(d) and Figs. S3, S4 (a), (b) show, where, at first,  $dV/dI$  increases with voltages at zero-bias. Hence, in our case, high (or more) conductive state (or LRS) corresponds to semimetallic  $1\text{T}^-$  or  $\text{T}_d$  phase and low conductive state (or HRS) with sharp zero-bias maximum in  $dV/dI$  is formed by applying a voltage, contrary to Zhang *et al.* [10]. It looks so that the intermediate state (something between 2H and  $1\text{T}^-$  or  $\text{T}_d$  states) can be formed by electric field both from 2H phase, as mentioned by Zhang *et al.* [10], or from  $\text{T}_d$  or  $1\text{T}^-$  phase as in our case. Note also that 2H –  $1\text{T}$  semiconductor–metal transition was observed in  $\text{MoTe}_2$  thin films under uniform tensile strain when the in-plane lattice constant between Te atoms is extended by  $\sim 3\%$  [12]. At the same time, our attempts to observe the switching starting from the semiconducting 2H-phase of  $\text{MoTe}_2$  ended in vain.

It seems likely that in our case high electric field in PC core (see Fig. 4(a)) produces some rearrangements of atomic structure. That is quite possible, given the fact that according to the recent observation, native metallicity and ferroelectricity can coexist in  $\text{MoTe}_2$  and  $\text{WTe}_2$  [13, 14, 15]. Yuan *et al.* [13] relate the origin of ferroelectricity in the  $\text{MoTe}_2$  monolayer to spontaneous symmetry breaking due to relative displacements of Mo atoms and Te atoms as a result of the formation of a distorted d1T phase. They constructed ferroelectric tunneling junction on the base of  $\text{MoTe}_2$  monolayer and measured highly nonlinear  $I$ - $V$  curve with the “on/off” resistance ratio of about 1000 at room temperature, where two polarization directions stand for the “on” and “off” states and ferroelectric switching can be induced by an electric field. Further, Fei *et al.* [14] observed that two- or three-layer  $\text{WTe}_2$  exhibits spontaneous out-of-plane

electric polarization that can be switched using gate electrodes and the polarization states can be differentiated by their conductivity. Moreover, Sharma *et al.* [15] provide evidence that native metallicity and ferroelectricity coexist also in bulk crystalline  $\text{WTe}_2$ , calling it “A room-temperature ferroelectric semimetal”. They have also demonstrated that  $\text{WTe}_2$  has switchable spontaneous polarization and natural ferroelectric domains with a distorted circular profile with an average domain size of  $\sim 20$  to  $50$  nm. That is, ferroelectricity is a bulk property of  $\text{WTe}_2$  and is not limited to few-layer samples only. Therefore, we assume that when relative atomic displacements of Mo atoms and Te atoms produces polarization (in other words electric field), then inverse effect must also take place. Namely, high electric field in PC can induce mentioned atomic displacement that leads to the phase transition and/or appearance of domain in PC (see Fig. 4(a)) with different properties. In this case, the new phase (something like distorted d1T) must manifest semiconducting like behavior. Then, observed switching in PCs can be due to reversible phase transition in the formed domain between distorted/intermediate (maybe d1T) and semimetallic  $T_d$  or 1T' phase triggered by high electric field.

Considering also that the title materials belong to the family of Weyl semimetals with topologically protected surface states, the discovery and exploitation of specific properties of these surface states in homo/hetero-structures is of a great challenge. Recall that the investigated materials have the same  $T_d$  crystal structure at low temperatures, which has broken inversion symmetry. It results in an uncompensated dipole, resulting in polarization along the c-axis, which can exist in the  $T_d\uparrow$  and  $T_d\downarrow$  states due to the asymmetric Te bonding environments [16]. Imagine, that under the action of high electric field a domain (see Fig. 4(a)) has a certain polarization, let's say  $T_d\uparrow$ . Therefore, a high electric field of opposite polarity can flip the dipole moment of domain with the corresponding change of the crystal structure from  $T_d\uparrow$  to  $T_d\downarrow$ . The interface between  $T_d\uparrow$  and  $T_d\downarrow$  is 1T' phase (see Fig. 4(b)). Thus, the electron scattering on the domain wall between  $T_d\uparrow$  and  $T_d\downarrow$  phase with specific surface states can lead to the increased resistance and simulate HRS behavior. Of course, this model requires sophisticated theoretical calculations, that have not yet been completed.

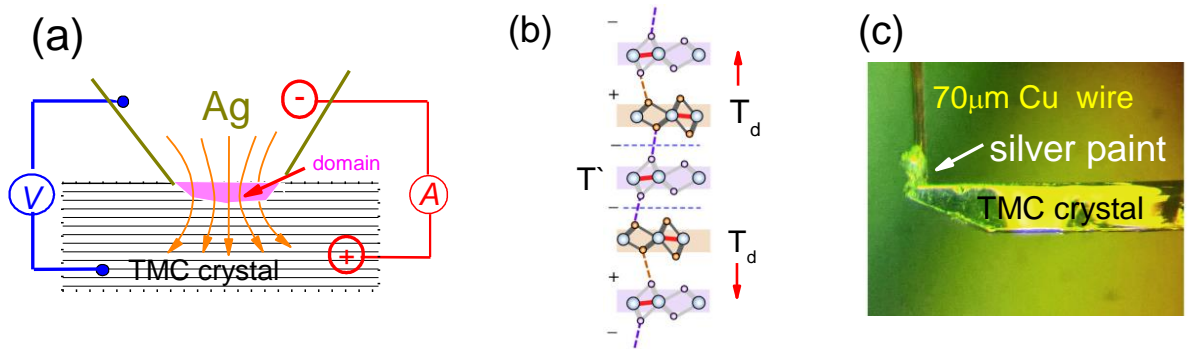


**Figure 4.** Representation of point contact. (a) Model of PC between TMC crystal and Ag showing current and voltage leads and “active region”, where an electric field is maximal. Arrows show spreading of a current in PC. (b) schematic model of domain wall between  $T_d\uparrow$  and  $T_d\downarrow$  states containing one 1T' unit as bridge according to [16]. (c) Photo image of “soft” PC, where silver paint touches the sample and connects to a thin Cu wire  $\varnothing 70\mu\text{m}$ .

## Conclusion and outlook

We report the discovery of a resistive switching in PCs based on series of TMC compounds such as  $\text{MeTe}_2$  ( $\text{Me}=\text{Mo}, \text{W}$ ) and  $\text{TaMeTe}_4$  ( $\text{Me}=\text{Ru}, \text{Rh}, \text{Ir}$ ). The switching effect consists of, up to two orders of magnitude change in the PC resistance, which increases with lowering of temperature. The origin of the effect is likely due to reversible modification of the crystal/electronic structure of TMC and creation of domain in PC under the application of high electric field. As a result, the transition takes place between the low resistive metallic and the



high resistive semiconducting-type states depending on domain properties. Besides, presence of domain walls with topological interfacial states can also play a role. Because of used manual method of device preparation at ambient condition, scattering in device parameters, e.g., such as shown in Fig. 3, is not surprising. On the other hand, this suggests that by using modern nanofabrication technologies of such structure formation, the device parameters can be sufficiently improved. Undoubtedly, such a simple method of device preparation has a great advantage in finding suitable materials for modern nanoelectronics application. It worth noting here, that the first observation of the resistive switching effect, e.g., in strongly correlated high- $T_c$  materials [17] and manganese-based perovskite oxides with colossal magnetoresistance [18], was also observed by using of PC technique, demonstrating its capabilities. Summing up, our observation of the resistive switching effect in series of TMC compounds expands significantly the range of materials promising for RRAM development [10, 19], for ferroelectric phase change transistors [20], for other nanoelectronic applications [21] and opens a straight path for discovering the effect in other metallic layered materials, what paves the way to electronics with new improbable functionalities. On the other hand, the understanding underlying physics of the switching processes is of great importance, which can open the avenue to the use of topological surface states at interface in different applications.

## Methods

**Synthesis.** Bulk single crystals of  $\text{MoTe}_2$ ,  $\text{WTe}_2$  and other TMC were grown with Te flux. To avoid contamination, the mixing and weighting were carried out in an Ar-filled glove box. Amounts of 0.5 g of Mo, W powder and 10 g Te were mixed and placed in an evacuated quartz ampoule. The ampoule was placed in a box furnace and slowly heated to 1000 °C and cooled down slowly to 800 °C followed by a hot centrifuge to remove the excess Te-flux. Single crystals were grown having a needle-like shape with a layered morphology. The as-grown crystals were characterized by SEM in EDX mode for compositional analysis and by x-ray diffraction for structural analysis. More details of the crystal growth and characterization are reported in Refs. [22, 23].

**Point contact spectroscopy.** PCs were prepared by touching of a thin Ag wire to a cleaved at room temperature flat surface of TMC needle-like single-crystal flake or contacting the edge of a plate-like sample by this wire. So-called “soft” PCs made by dripping of a small drop of silver paint onto the cleaved TMC surface/edge (see Fig. 4(c)). The latter type of PCs demonstrates better stability versus temperature change. Thus, we conducted resistive measurements on the heterocontacts between a normal metal (Ag or silver paint) and the TMC. We measured current–voltage characteristics  $I$ – $V$  of PCs and their first derivatives  $dV/dI(V)$ . The first derivative or differential resistance  $dV/dI(V) \equiv R(V)$  was recorded by sweeping the dc current  $I$  on which a small ac current  $i$  was superimposed using a standard lock-in technique. The measurements were performed in the temperature range from liquid helium up to the room temperature.

## Acknowledgments

We thank A. V. Terekhov and S. Gaß for the technical assistance. This work was financially supported by the Volkswagen Foundation in the frame of Trilateral Initiative. YGN, DLB and OEK are grateful for support by the National Academy of Sciences of the Ukraine under project Φ4-19 and would like to thank the IFW Dresden for hospitality. Support by Deutsche Forschungsgemeinschaft (DFG) through Grant No: AS 523/4-1 is acknowledged. SA & BB also acknowledge support of DFG through Projekt No: 405940956.

## References

- [1] Manzeli S *et al* 2017 2D transition metal dichalcogenides *Nat. Rev. Mater.* **2** 17033
- [2] Yan B and Felser C 2017 Topological Materials: Weyl Semimetals *Annu. Rev. Condens. Matter Phys.* **8** 337

- [3] Wang Q H *et al* 2012 Electronics and optoelectronics of two-dimensional transition metal dichalcogenides *Nature Nanotechnol.* **7** 699
- [4] Naidyuk Yu *et al* 2018 Surface superconductivity in the Weyl semimetal MoTe<sub>2</sub> detected by point contact spectroscopy *2D Mater.* **5** 045014
- [5] Naidyuk Yu G *et al* 2019 Yanson point-contact spectroscopy of Weyl semimetal WTe<sub>2</sub> *2D Mater.* **6** 045012
- [6] Naidyuk Yu G and Yanson I K 2005 Point-Contact Spectroscopy, *Springer Series in Solid-State Sciences* vol 145 (New York: Springer)
- [7] Verkin B I *et al* 1979 Singularities in  $d^2V/dI^2$  dependences of point contacts between ferromagnetic metals *Solid State Commun.* **30** 215
- [8] Clarke R Marsegilia E and Hughes H P 1978 A low-temperature structural phase transition in  $\beta$ -MoTe<sub>2</sub> *Philos. Mag.* **38** 121
- [9] Cao Chuanwu *et al* 2018 Barkhausen effect in the first order structural phase transition in type-II Weyl semimetal MoTe<sub>2</sub> *2D Mater.* **5** 044003
- [10] Zhang F *et al* 2019 Electric-field induced structural transition in vertical MoTe<sub>2</sub>-and Mo<sub>1-x</sub>W<sub>x</sub>Te<sub>2</sub>-based resistive memories *Nat. Mater.* **18** 55
- [11] Datye I *et al* 2020 Localized Heating and Switching in MoTe<sub>2</sub>-Based Resistive Memory Devices *Nano Lett.* **20** 1461
- [12] Song S *et al* 2016 Room temperature semiconductor–metal transition of MoTe<sub>2</sub> thin films engineered by strain *Nano Lett.* **16** 188.
- [13] Fei Z *et al* 2018 Ferroelectric switching of a two-dimensional metal *Nature* **560** 336
- [14] Yuan S *et al* 2019 Room-temperature ferroelectricity in MoTe<sub>2</sub> down to the atomic monolayer limit *Nat. Commun.* **10** 1775
- [15] Sharma P *et al* 2019 A room-temperature ferroelectric semimetal *Sci. Adv.* **5**, eaax5080
- [16] Fei-Ting Huang *et al* 2019 Polar and phase domain walls with conducting interfacial states in a Weyl semimetal MoTe<sub>2</sub> *Nat. Commun.* **10** 4211
- [17] Rybaltchenko L F *et al* 1999 Reversible transitions in high-T<sub>c</sub> cuprates based point contacts *European Physical Journal B* **10** 475.
- [18] Belogolovskii M A *et al* 2002 Inelastic electron tunneling across magnetically active interfaces in cuprate and manganite heterostructures modified by electromigration processes *Low Temp. Phys.* **28** 391
- [19] Zhao Q *et al* 2020 Current Status and Prospects of Memristor Based on Novel 2D Materials. *Mater. Horiz.* **7** 1495
- [20] Hou W *et al* 2019 Strain-based room-temperature non-volatile MoTe<sub>2</sub> ferroelectric phase change transistor *Nat. Nanotech.* **14** 668
- [21] Su J *et al* 2019 Van der Waals 2D Transition Metal Tellurides *Adv. Mater. Interfaces* **6** 1900741
- [22] Pawlik A-S *et al* 2018 Thickness dependent electronic structure of exfoliated mono- and few-layer 1T'-MoTe<sub>2</sub> *Phys. Rev. Materials* **2** 104004
- [23] Shipunov G *et al* (in preparation)



# Supplement

to the paper by Naidyuk et al.:

## “Switchable topological domains in point contacts based on transition metal tellurides”

1) Examples of resistive switching in PCs with TaRhTe<sub>4</sub> and TaRuTe<sub>4</sub> compounds.

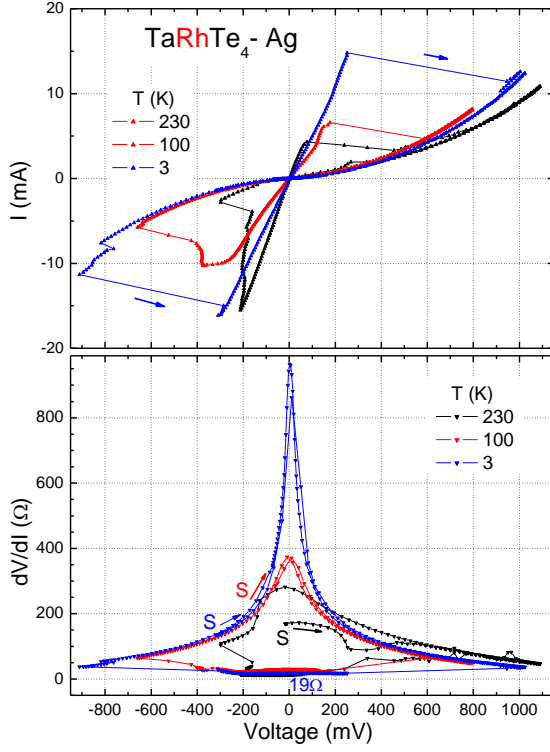


**Figure S1.** Upper panel:  $I$ - $V$  curves of “soft” PC TaRhTe<sub>4</sub>-Ag measured at different temperatures. Bottom panel:  $dV/dI$  of the same “soft” PC.”s” marks the start of measurements from HRS. PC resistance is 19 Ohm in LRS at 3K.

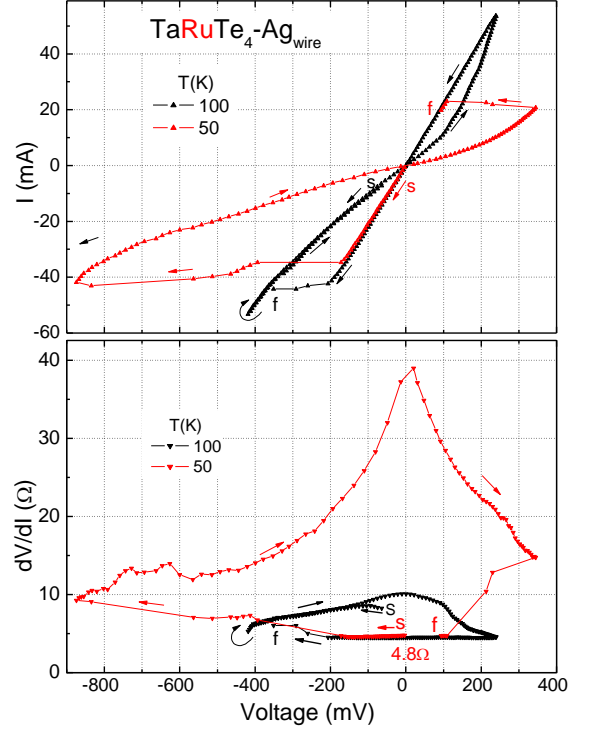


**Figure S2.** Upper panel:  $I$ - $V$  curves of “hard” PC TaRuTe<sub>4</sub>-Ag measured at two temperatures. Bottom panel:  $dV/dI$  of the same “hard” PC.”s” marks the start of measurement and “f” is the finish, arrows show direction of the current sweep. PC resistance is 4.8 Ohm in LRS at 50K.

2) Examples of resistive switching in “hard” PCs and in low-ohmic “soft” PC.

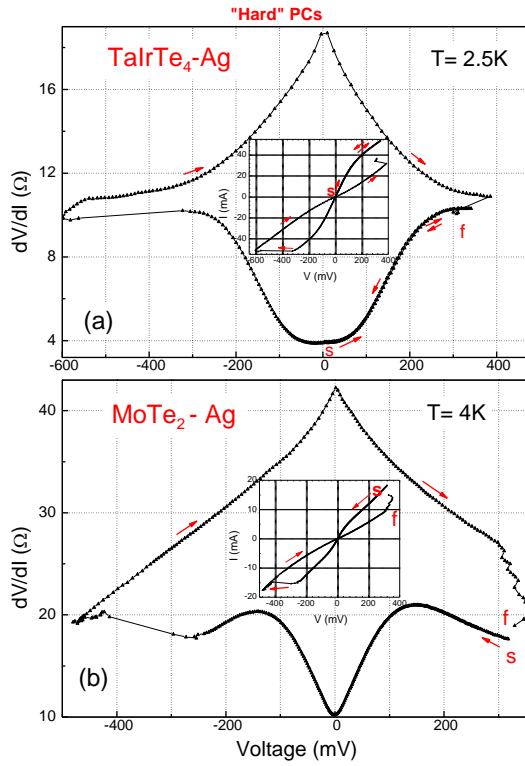


**Figure S3.**  $dV/dI$  of two “hard” PCs made by mechanical contact of thin  $70\text{ }\mu\text{m}$  Ag wire to  $\text{TaIrTe}_4$  and  $\text{MoTe}_2$  crystals at helium temperature. Insets show  $I$ - $V$  characteristics for same PCs from the main panels.

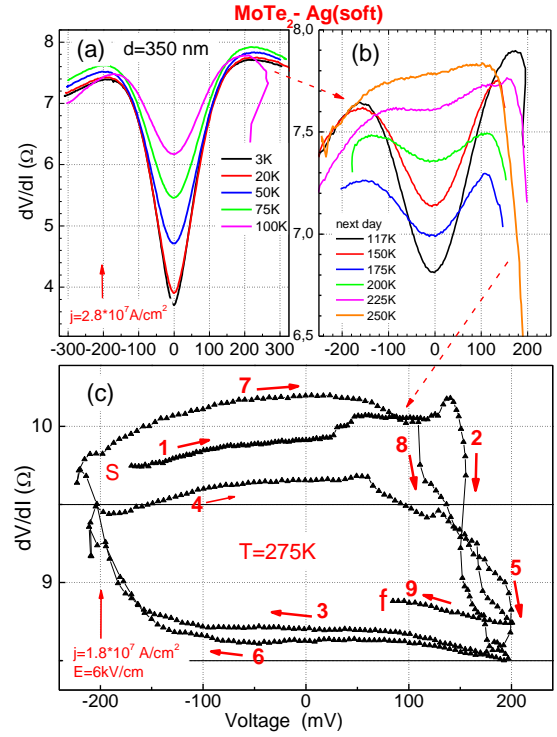


**Figure S4.** (a), (b) Evolution of  $dV/dI$  of  $\text{MoTe}_2$  “soft” contact with temperature. Here a sharp decline of  $dV/dI$  at a positive voltage may indicate the start of switching. (c)  $dV/dI$  of the same contact with switching effect successively measured “clock-wise” repeatedly at  $275\text{K}$ . The diameter of this contact was estimated as  $350\text{ nm}$  using the temperature dependence of their zero bias resistance. Strength of the electric field and the current density were estimated at LRS to HRS transition as shown by vertical arrows.

### 3) Details of $dV/dI$ and $dI/dV$ behavior in PCs.

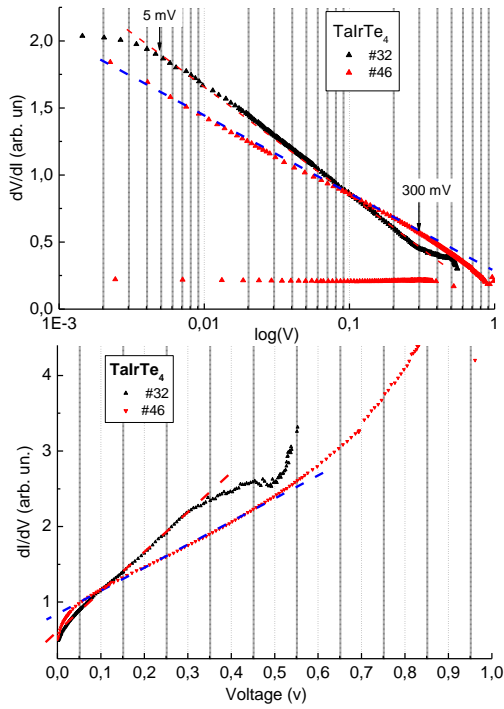


**Figure S5.** Upper panel:  $dV/dI$  curves of two “soft” PCs TaIrTe<sub>4</sub>-Ag from Fig. 1(a) in log-scale. Bottom panel:  $dI/dV$  for the same PCs. The dash lines in the figures are guide for the eye.

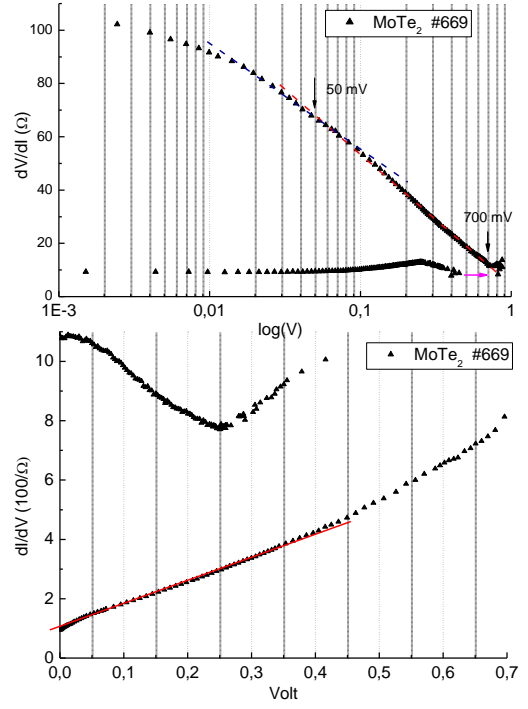


**Figure S6.** Upper panel:  $dV/dI$  curves of “soft” PC MoTe<sub>2</sub>-Ag from Fig 2 in log-scale. Bottom panel:  $dI/dV$  for the same PC. The dash lines in the figures are guide for the eye.

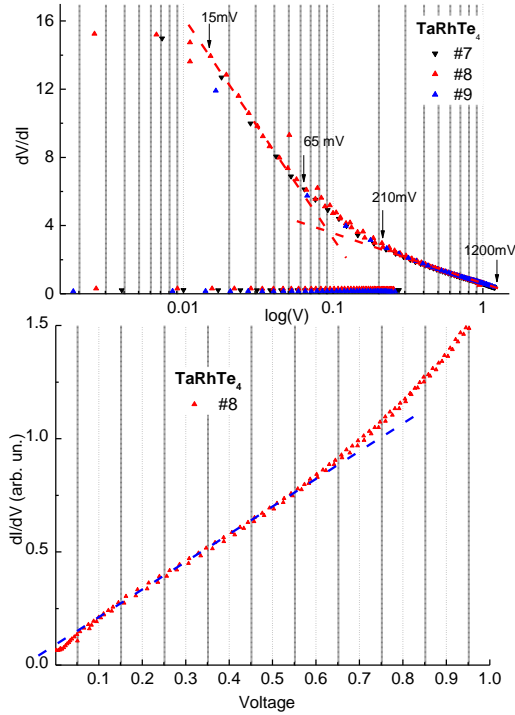


**Figure S7.** Upper panel:  $dV/dI$  curves of “soft” PC TaRhTe<sub>4</sub>-Ag for three successive sweeps (different symbols) in log-scale. Bottom panel:  $dI/dV$  for the same PC. The dash lines in the figures are guide for the eye.

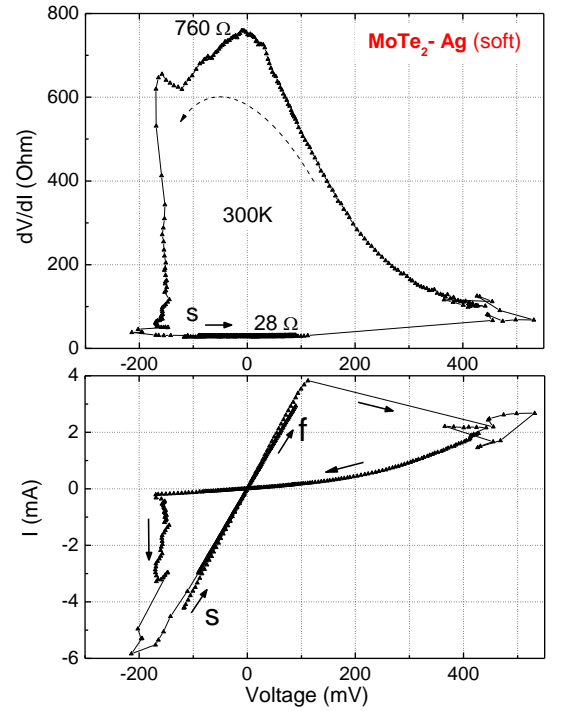


**Figure S8.** Differential resistance  $dV/dI$  and  $I$ - $V$  curves behavior for soft contact based on MoTe<sub>2</sub> at room temperature.